Title	Three-dimensional vibration analysis of a torus with circular cross section
Author(s)	Zhou, D; Au, FTK; Lo, SH; Cheung, YK
Citation	Journal Of The Acoustical Society Of America, 2002, v. 112 n. 6, p. 2831-2839
Issued Date	2002
URL	http://hdl.handle.net/10722/42648
Rights	Creative Commons: Attribution 3.0 Hong Kong License

Three-dimensional vibration analysis of a torus with circular cross section

D. Zhou
Department of Mechanics and Engineering Science, Nanjing University of Science and Technology, Nanjing 210014, People's Republic of China

F. T. K. Au, S. H. Lo, and Y. K. Cheung[a)]
Department of Civil Engineering, The University of Hong Kong, Hong Kong, People's Republic of China

(Received 28 November 2001; revised 3 August 2002; accepted 4 August 2002)

The free vibration characteristics of a torus with a circular cross section are studied by using the three-dimensional, small-strain, elasticity theory. A set of three-dimensional orthogonal coordinates system, comprising the polar coordinate (r,θ) at each circular cross section and the circumferential coordinate φ around the ring, is developed. Each of the displacement components u_r, v_θ, and w_φ in the r, θ, and φ directions, respectively, is taken as a product of the Chebyshev polynomials in the r direction and the trigonometric functions in the θ and φ directions. Eigenfrequencies and vibration mode shapes have been obtained via a three-dimensional displacement-based extremum energy principle. Upper bound convergence of the first seven eigenfrequencies accurate to at least six significant figures is obtained by using only a few terms of the admissible functions. The eigenfrequency responses due to variation of the ratio of the radius of the ring centroidal axis to the cross-sectional radius are investigated in detail. Very accurate eigenfrequencies and deformed mode shapes of the three-dimensional vibration are presented. All major modes such as flexural thickness-shear modes, in-plane stretching modes, and torsional modes are included in the analysis. The results may serve as a benchmark reference for validating other computational techniques for the problem. © *2002 Acoustical Society of America.* [DOI: 10.1121/1.1509429]

PACS numbers: 43.40.−r, 43.40.Cw, 43.40.At [ANN]

I. INTRODUCTION

A torus (circular ring beam with circular cross section) as basic structural element can find its applications in civil, mechanical, aircraft, and marine engineering like gyroscopes, springs, stiffeners and tires, etc. In some cases, the torus has to bear dynamic loads, and therefore to understand its dynamic behavior is very important for designers. One-dimensional mathematical models about rings have been available for more than a century.[1,2] Considering the ring as a curved beam or rod, the vibration of a ring can be classified as in-plane, out-of-plane, and circumferential modes. Based on the classical theory (i.e., the hypothesis of a straight normal line), three uncoupled differential equations can be developed for these three modes and solved easily if the extension of the centerline of the ring is negligible. In order to improve the classical solutions, some investigators[3–6] have studied the effect of extension, transverse shear, and rotary inertia.

The existing research work shows that for rings with a circular cross section, the error of the one-dimensional models increases with the decrease of the ratio of ring centroidal-axis radius to cross-sectional radius. Similar conclusions can also be drawn for rings with a cross section of any shape. In addition to the one-dimensional models, sometimes investigators also applied two-dimensional plate[7,8] and shell[9,10] models to analyze the mechanical behavior of a torus. According to a recent literature survey,[11] most of the published papers are about rings with a rectangular cross section. For rings with a circular cross section, only the one-dimensional models have been developed. It is well known that these mathematical models have serious limitations in their scope of applications, which are only suitable for slender or thin structural elements. As a result, the three-dimensional analysis of structural elements has long been a goal of those who work in the field. In the recent two decades, with the development of digital computers and computational techniques, it has now become possible to obtain accurate eigenfrequencies and vibration mode shapes for some structural elements. Exact, closed-form three-dimensional elasticity solutions can be obtained only for a few cases, such as the axisymmetric vibration of annular plates,[12] and the vibration of rectangular plates with four simply supported edges.[13] Using a series expansion method, accurate solutions for the free vibration of circular plates and cylinders have been derived by Hutchinson.[14–18] In recent years, the Ritz method has been extensively applied to the three-dimensional vibration analysis of some typical structural elements, such as beams with a circular cross section,[19] circular plates[20,21] and cylindrical shells,[22,23] rectangular and trapezoidal plates,[24,25] prismatic columns,[26] shell panels,[27,28] triangular plates,[29,30] and rings with isosceles trapezoidal and triangular cross sections,[31] etc. In these references, high accuracy, a small computational cost, and easy coding preparation have been shown if suitable admissible functions are selected.

In the present work, the Ritz method is applied to the free vibration analysis of a torus with a circular cross section

a)Author to whom correspondence should be addressed. Electronic mail: hreccyk@hkucc.hku.hk

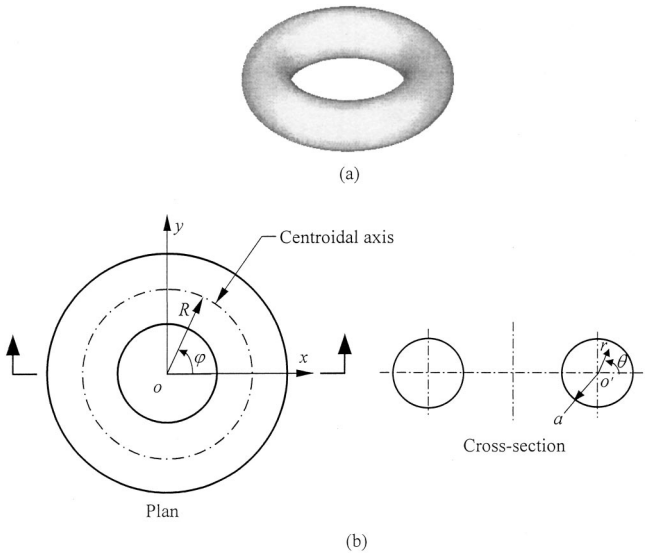

FIG. 1. A torus with a circular cross section: (a) three-dimensional view; (b) coordinate system.

based on the three-dimensional elasticity theory. Although the method itself does not guarantee us to provide exact solutions, high accuracy and quick convergence may be achieved if one selects the displacement functions properly. In this paper, a combination of the polar coordinate (r,θ) at each circular cross section and the circumferential coordinate φ around the ring, is developed to describe the strain and stress distributions in the torus. The corresponding displacement components are taken to be u_r, ν_θ, and w_φ in the r, θ, and φ directions, respectively. Each displacement component is expressed as a product of three separable coordinate functions: a series of Chebyshev polynomials in the r coordinate and a series of trigonometric functions in the θ and φ coordinates. It is obvious that each displacement function is composed of orthogonal and complete series in the region because each component function is orthogonal and complete. Therefore, the eigenfrequencies presented in this work are very accurate and often accurate to at least six significant figures. They can therefore serve as a benchmark solution for the one-dimensional ring theory and future computational techniques for the problem.

II. THEORETICAL FORMULATION

Consider a torus with a circular cross section, as shown in Fig. 1. The cross-sectional radius of the ring is a and the centroidal-axis radius of the ring is R $(R>a)$. A combination of the polar coordinate (r,θ) at each cross section and the circumferential coordinate φ around the ring is chosen to describe the strain and stress in the torus. The polar coordinate with an origin at the centroidal axis of the ring is used to describe the stress and strain at the cross section. The circumferential coordinate with an origin at the center of the torus is used to describe those quantities along the direction normal to the cross section. It is obvious that the three coordinates (r,θ,φ) in this set of curved coordinate system are orthogonal to each other. The transformation relations between the Cartesian coordinates and the present curved coordinates are given as follows:

$$\begin{aligned} &x=(R+r\cos\theta)\cos\varphi; \quad y=(R+r\cos\theta)\sin\varphi;\\ &z=r\sin\theta. \end{aligned} \tag{1}$$

Let u, ν, and w, respectively, be the displacements in r, θ, and φ directions. The relations between three-dimensional tensorial strains and displacement components in the orthogonal curved coordinate system are given by

$$\begin{aligned} &\epsilon_r=\frac{\partial u}{\partial r}; \quad \epsilon_\theta=\frac{1}{r}\frac{\partial \nu}{\partial\theta}+\frac{u}{r};\\ &\epsilon_\varphi=\frac{1}{R+r\cos\theta}\frac{\partial w}{\partial\varphi}+\frac{\cos\theta}{R+r\cos\theta}u-\frac{\sin\theta}{R+r\cos\theta}\nu;\\ &\gamma_{r\theta}=\frac{\partial\nu}{\partial r}-\frac{\nu}{r}+\frac{1}{r}\frac{\partial u}{\partial\theta};\\ &\gamma_{\theta\varphi}=\frac{1}{r}\frac{\partial w}{\partial\theta}+\frac{\sin\theta}{R+r\cos\theta}w+\frac{1}{R+r\cos\theta}\frac{\partial\nu}{\partial\varphi};\\ &\gamma_{\varphi r}=\frac{1}{R+r\cos\theta}\frac{\partial u}{\partial\varphi}+\frac{\partial w}{\partial r}-\frac{\cos\theta}{R+r\cos\theta}w. \end{aligned} \tag{2}$$

From Eq. (1), the determinant of the Jacobian matrix of the coordinate system is given by

$$|J|=r(R+r\cos\theta). \tag{3}$$

Therefore, the strain energy V and the kinetic energy T of the torus undergoing free vibration are

$$\begin{aligned} V=(1/2)\int_0^{2\pi}\int_0^{2\pi}\int_0^a[&(\lambda+2G)\epsilon_r^2+2\lambda\epsilon_r\epsilon_\theta+2\lambda\epsilon_r\epsilon_\varphi\\ &+(\lambda+2G)\epsilon_\theta^2+2\lambda\epsilon_\theta\epsilon_\varphi+(\lambda+2G)\epsilon_\varphi^2\\ &+G(\gamma_{r\theta}^2+\gamma_{\theta\varphi}^2+\gamma_{\varphi r}^2)]|J|dr\,d\theta\,d\varphi;\\ T=(\rho/2)\int_0^{2\pi}\int_0^{2\pi}\int_0^a&(\dot u+\dot\nu+\dot w)|J|dr\,d\theta\,d\varphi, \end{aligned} \tag{4}$$

where ρ is the constant mass per unit volume; $\dot u$, $\dot\nu$, and $\dot w$ are the velocity components. The parameters λ and G are the Lamé constants for a homogeneous and isotropic material, which are expressed in terms of Young's modulus E and the Poisson's ratio ν by

$$\lambda=\nu E/[(1+\nu)(1-2\nu)]; \quad G=E/[2(1+\nu)]. \tag{5}$$

In free vibrations, the displacement components may be expressed as

$$\begin{aligned} &u=U(r,\theta,\varphi)e^{i\omega t}; \quad \nu=V(r,\theta,\varphi)e^{i\omega t};\\ &w=W(r,\theta,\varphi)e^{i\omega t}, \end{aligned} \tag{6}$$

where ω is the circular eigenfrequency of the torus and $i=\sqrt{-1}$.

Considering the circumferential symmetry of the torus about the coordinate φ, the displacement functions can be expressed as

$$U(r,\theta,\varphi)=\overline{U}(r,\theta)\cos(n\varphi);$$
$$V(r,\theta,\varphi)=\overline{V}(r,\theta)\cos(n\varphi); \tag{7}$$
$$W(r,\theta,\varphi)=\overline{W}(r,\theta)\sin(n\varphi),$$

where n is the circumferential wave number that should be an integer, i.e., $n=0,1,2,3,\ldots,\infty$ to ensure periodicity. It is obvious that $n=0$ denotes the axisymmetric modes. Rotating the axes of symmetry, another set of free vibration modes can be obtained, which corresponds to an interchange of $\cos(n\varphi)$ and $\sin(n\varphi)$ in Eq. (7). However, in such a case, $n=0$ means $U(r,\theta,\varphi)=0$, $V(r,\theta,\varphi)=0$ and $W(r,\theta,\varphi)=\overline{W}(r,\theta)$, which corresponds to the torsional modes.

Defining the following dimensionless coordinates:

$$\overline{R}=R/a; \quad \overline{r}=r/a, \tag{8}$$

and then substituting Eqs. (6) and (7) into Eq. (4), gives

$$\begin{aligned} V_{\max}=&(Ga/2)\int_0^{2\pi}\int_0^1[(\overline{\lambda}+2)\overline{\epsilon}_r^2+2\overline{\lambda}\overline{\epsilon}_r\overline{\epsilon}_\theta+2\overline{\lambda}\overline{\epsilon}_r\overline{\epsilon}_\varphi \\ &+(\overline{\lambda}+2)\overline{\epsilon}_\theta^2+2\overline{\lambda}\overline{\epsilon}_\theta\overline{\epsilon}_\varphi+(\overline{\lambda}+2)\overline{\epsilon}_\varphi^2+\overline{\gamma}_{r\theta}^2+\overline{\gamma}_{\theta\varphi}^2 \\ &+\overline{\gamma}_{\varphi r}^2]\overline{r}(\overline{R}+\overline{r}\cos\theta)d\overline{r}\,d\theta; \\ T_{\max}=&(\rho a^3\omega^2/2)\int_0^{2\pi}\int_0^1(\Gamma_1\overline{U}^2+\Gamma_1\overline{V}^2+\Gamma_2\overline{W}^2) \\ &\times\overline{r}(\overline{R}+\overline{r}\cos\theta)d\overline{r}\,d\theta, \end{aligned} \tag{9}$$

in which

$$\overline{\lambda}=\frac{2\nu}{1-2\nu}; \quad \overline{\epsilon}_r^2=\Gamma_1\left(\frac{\partial\overline{U}}{\partial\overline{r}}\right)^2;$$
$$\overline{\epsilon}_\theta^2=\frac{\Gamma_1}{\overline{r}^2}\left[\left(\frac{\partial\overline{V}}{\partial\theta}\right)^2+2\overline{U}\frac{\partial\overline{V}}{\partial\theta}+\overline{U}^2\right];$$
$$\begin{aligned}\overline{\epsilon}_\varphi^2=&\frac{\Gamma_1}{(\overline{R}+\overline{r}\cos\theta)^2}[n^2\overline{W}^2+2n\cos\theta\overline{U}\overline{W}-2n\sin\theta\overline{V}\overline{W} \\ &+\cos^2\theta\overline{U}^2-\sin(2\theta)\overline{U}\overline{V}+\sin^2\theta\overline{V}^2];\end{aligned}$$
$$\overline{\epsilon}_r\overline{\epsilon}_\theta=\frac{\Gamma_1}{\overline{r}}\left(\frac{\partial\overline{U}}{\partial\overline{r}}\frac{\partial\overline{V}}{\partial\theta}+\overline{U}\frac{\partial\overline{U}}{\partial\overline{r}}\right);$$
$$\begin{aligned}\overline{\epsilon}_\theta\overline{\epsilon}_\varphi=&\frac{\Gamma_1}{\overline{r}(\overline{R}+\overline{r}\cos\theta)}\left[n\left(\frac{\partial\overline{V}}{\partial\theta}\overline{W}+\overline{U}\overline{W}\right)\right. \\ &\left.+\cos\theta\left(\overline{U}\frac{\partial\overline{V}}{\partial\theta}+\overline{U}^2\right)-\sin\theta\left(\overline{V}\frac{\partial\overline{V}}{\partial\theta}+\overline{U}\overline{V}\right)\right];\end{aligned} \tag{10}$$
$$\overline{\epsilon}_\varphi\overline{\epsilon}_r=\frac{\Gamma_1}{\overline{R}+\overline{r}\cos\theta}\left[n\frac{\partial\overline{U}}{\partial\overline{r}}\overline{W}+\cos\theta\overline{U}\frac{\partial\overline{U}}{\partial\overline{r}}-\sin\theta\frac{\partial\overline{U}}{\partial\overline{r}}\overline{V}\right];$$
$$\begin{aligned}\gamma_{r\theta}^2=&\Gamma_1\left[\left(\frac{\partial\overline{V}}{\partial\overline{r}}\right)^2-\frac{2}{\overline{r}}\overline{V}\frac{\partial\overline{V}}{\partial\overline{r}}+\frac{2}{\overline{r}}\frac{\partial\overline{U}}{\partial\theta}\frac{\partial\overline{V}}{\partial\overline{r}}+\frac{1}{\overline{r}^2}\overline{V}^2\right. \\ &\left.-\frac{2}{\overline{r}^2}\frac{\partial\overline{U}}{\partial\theta}\overline{V}+\frac{1}{\overline{r}^2}\left(\frac{\partial\overline{U}}{\partial\theta}\right)^2\right];\end{aligned}$$
$$\begin{aligned}\gamma_{\theta\varphi}^2=&\Gamma_2\left[\frac{1}{\overline{r}^2}\left(\frac{\partial\overline{W}}{\partial\theta}\right)^2+\frac{2}{\overline{r}(\overline{R}+\overline{r}\cos\theta)}\right. \\ &\times\left(\sin\theta\overline{W}\frac{\partial\overline{W}}{\partial\theta}-n\overline{V}\frac{\partial\overline{W}}{\partial\theta}\right)+\frac{1}{(\overline{R}+\overline{r}\cos\theta)^2} \\ &\left.\times(\sin^2\theta\overline{W}^2-2n\sin\theta\overline{V}\overline{W}+n^2\overline{V}^2)\right];\end{aligned}$$
$$\begin{aligned}\gamma_{\varphi r}^2=&\Gamma_2\left[\left(\frac{\partial\overline{W}}{\partial\overline{r}}\right)^2-\frac{2}{(\overline{R}+\overline{r}\cos\theta)}\right. \\ &\times\left(\cos\theta\overline{W}\frac{\partial\overline{W}}{\partial\overline{r}}+n\overline{U}\frac{\partial\overline{W}}{\partial\overline{r}}\right)+\frac{1}{(\overline{R}+\overline{r}\cos\theta)^2} \\ &\left.\times(n^2\overline{U}^2+2n\cos\theta\overline{U}\overline{W}+\cos^2\theta\overline{W}^2)\right],\end{aligned}$$

where

$$\Gamma_1=\int_0^{2\pi}\cos^2 n\varphi\,d\varphi=\begin{cases}2\pi, & \text{if } n=0,\\ \pi, & \text{if } n\geqslant 1,\end{cases}$$
$$\Gamma_2=\int_0^{2\pi}\sin^2 n\varphi\,d\varphi=\begin{cases}0, & \text{if } n=0,\\ \pi, & \text{if } n\geqslant 1.\end{cases} \tag{11}$$

The Lagrangian energy functional Π is given as

$$\Pi=T_{\max}-V_{\max}. \tag{12}$$

The displacement functions $\overline{U}(\overline{r},\theta)$, $\overline{V}(\overline{r},\theta)$, and $\overline{W}(\overline{r},\theta)$ are approximately expressed in terms of a finite series as

$$\overline{U}(\overline{r},\theta)=\sum_{i=1}^{I}\sum_{j=1}^{J}A_{ij}F_i(\overline{r})G_j(\theta);$$
$$\overline{V}(\overline{r},\theta)=\sum_{l=1}^{L}\sum_{m=1}^{M}B_{lm}F_l(\overline{r})\overline{G}_m(\theta); \tag{13}$$
$$\overline{W}(\overline{r},\theta)=\sum_{p=1}^{P}\sum_{q=1}^{Q}C_{pq}F_p(\overline{r})G_q(\theta),$$

where A_{ij}, B_{lm}, and C_{pq} are undetermined coefficients and I, J, L, M, P, and Q are the truncated orders of their corresponding series. It is obvious that if $F_i(\overline{r})$ $(i=1,2,3,\ldots,\infty)$, $G_j(\theta)$ $(j=1,2,3,\ldots,\infty)$ and $\overline{G}_m(\theta)$ $(m=1,2,3,\ldots,\infty)$ are all sets of mathematically complete series, then these three sets are capable of describing any three-dimensional motion of the torus. Therefore, as sufficient terms are taken, the results will approach the exact solutions as closely as desired.

TABLE I. Convergence of eigenfrequencies of a torus with a circular cross section when $\bar{R}=1.5$ and $n=1$.

Terms	Ω_1	Ω_2	Ω_3	Ω_4	Ω_5	Ω_6	Ω_7
			Symmetric modes about the centroidal-axis plane				
4×4	1.185 76	2.334 75	2.753 63	3.049 33	3.508 54	3.732 38	3.837 33
5×5	**1.185 74**	2.334 06	2.753 26	3.048 28	3.503 98	3.729 11	3.831 64
6×6	1.185 74	**2.334 04**	**2.723 21**	3.048 15	3.503 39	3.728 47	3.831 07
7×7	1.185 74	2.334 04	2.753 21	**3.048 14**	3.503 38	**3.728 44**	**3.831 05**
8×8	1.185 74	2.334 04	2.753 21	3.048 14	**3.503 37**	3.728 44	3.831 05
9×9	1.185 74	2.334 04	2.753 21	3.048 14	3.503 37	3.728 44	3.831 05
			Antisymmetric modes about the centroidal-axis plane				
4×4	1.155 46	2.143 68	2.492 66	3.108 78	3.473 95	3.778 32	4.629 33
5×5	1.155 07	**2.143 37**	2.492 04	3.108 55	3.470 28	3.772 59	4.549 37
6×6	1.155 04	2.143 37	**2.492 03**	**3.108 41**	**3.469 83**	3.771 67	4.545 57
7×7	**1.155 03**	2.143 37	2.492 03	3.108 41	3.469 83	3.771 65	**4.545 42**
8×8	1.155 03	2.143 37	2.492 03	3.108 41	3.469 83	**3.771 64**	4.545 42
9×9	1.155 03	2.143 37	2.492 03	3.108 41	3.469 83	3.771 64	4.545 42

Substituting Eqs. (10) and (13) into Eq. (9) and minimizing the Lagrangian functional Π with respect to the undetermined coefficients A_{ij}, B_{lm}, and C_{pq}, i.e.,

$$\frac{\partial}{\partial A_{ij}}(V_{\max}-T_{\max})=0 \quad (i=1,2,3,...,I;j=1,2,3,...,J);$$

$$\frac{\partial}{\partial B_{lm}}(V_{\max}-T_{\max})=0 \quad (l=1,2,3,...,L;m=1,2,3,...,M); \tag{14}$$

$$\frac{\partial}{\partial C_{pq}}(V_{\max}-T_{\max})=0 \quad (p=1,2,3,...,P;q=1,2,3,...,Q),$$

a set of eigenvalue equations is derived, which can be written in matrix form as

$$\left\{\begin{bmatrix} [K_{uu}] & [K_{u\nu}] & [K_{uw}] \\ & [K_{\nu\nu}] & [K_{\nu w}] \\ \text{symmetric} & & [K_{ww}] \end{bmatrix} - \Omega^2 \begin{bmatrix} [M_{uu}] & & \\ & [M_{\nu\nu}] & \\ & & [M_{ww}] \end{bmatrix}\right\} \begin{bmatrix} \{A\} \\ \{B\} \\ \{C\} \end{bmatrix} = \begin{bmatrix} \{0\} \\ \{0\} \\ \{0\} \end{bmatrix}, \tag{15}$$

in which $\Omega=\omega a\sqrt{\rho/G}$, $[K_{ij}]$ and $[M_{ii}]$ $(i,j=u,\nu,w)$ are, respectively, the stiffness submatrices and the diagonal mass submatrices, $\{A\}$, $\{B\}$, and $\{C\}$ are the column vectors of the unknown coefficients, respectively, corresponding to A_{ij} $(i=1,2,3,...I;\ j=1,2,3,...,J)$, B_{lm} $(l=1,2,...,L;\ m=1,2,3,...,M)$ and C_{pq} $(p=1,2,3,...,P;\ q=1,2,3,...,Q)$. A nontrivial solution is obtained by setting the determinant of the coefficient matrix of Eq. (15) to zero. The roots of the determinant are the square of the dimensionless eigenfrequencies (eigenvalues). The mode shapes (eigenfunctions) are determined by backsubstitution of the eigenvalues, one by one, in the usual manner.

It is noted that in using the Ritz method, the stress boundary conditions of the structure need not be satisfied in advance, but the geometric boundary conditions should be satisfied exactly. For a torus, there is actually no restraint on the surface displacements. In the present work, the Chebyshev polynomial series defined in the interval $[0, 1]$ and the trigonometric series defined in the interval $[0, 2\pi]$ are used as the admissible functions of displacements in the r and θ directions, respectively. It is obvious that a torus with a circular cross section is symmetric about the centroidal-axis plane (i.e., the plane containing the centroidal axis of the ring). Therefore, the vibration modes of the torus can be

TABLE II. The convergence of eigenfrequencies of a torus with a circular cross section when $\bar{R}=1.5$ and $n=5$.

Terms	Ω_1	Ω_2	Ω_3	Ω_4	Ω_5	Ω_6	Ω_7
			Symmetric modes about the centroidal-axis plane				
5×5	2.461 38	3.189 81	3.709 52	4.298 67	4.409 67	4.871 47	5.242 81
6×6	2.461 26	3.189 71	3.708 74	4.298 22	4.407 66	4.865 66	5.236 25
7×7	**2.461 24**	3.189 71	3.709 63	4.298 19	4.407 47	4.864 89	5.235 40
8×8	2.461 24	**3.189 70**	**3.709 61**	**4.298 18**	**4.407 44**	4.864 76	5.235 24
9×9	2.461 24	3.189 70	3.709 61	4.298 18	4.407 44	**4.864 74**	**5.235 21**
10×10	2.461 24	3.189 70	3.709 61	4.298 18	4.407 44	4.864 74	5.235 21
			Antisymmetric modes about the centroidal-axis plane				
5×5	2.163 12	3.156 36	3.772 63	4.307 75	4.688 60	5.106 18	5.472 98
6×6	2.163 08	3.156 21	3.771 99	4.306 44	4.685 39	5.103 40	5.436 34
7×7	**2.163 07**	**3.156 19**	3.771 91	4.306 38	4.684 98	5.103 10	5.435 22
8×8	2.163 07	3.156 19	**3.771 90**	**4.306 37**	4.684 92	**5.103 07**	5.435 14
9×9	2.163 07	3.156 19	3.771 90	4.306 37	**4.684 91**	5.103 07	**5.435 13**
10×10	2.163 07	3.156 19	3.771 90	4.306 37	4.684 91	5.103 07	5.435 13

TABLE III. The convergence of eigenfrequencies of axisymmetric vibration for a torus with circular cross section when $\bar{R}=1.5$.

Terms	Ω_1	Ω_2	Ω_3	Ω_4	Ω_5	Ω_6	Ω_7
			Symmetric modes about the centroidal-axis plane				
5×5	1.176 85	2.614 42	2.879 30	3.799 87	4.116 45	4.504 47	4.898 72
6×6	**1.176 82**	2.614 28	2.879 06	3.797 26	4.115 71	4.502 95	4.884 95
7×7	1.176 82	**2.614 26**	**2.879 04**	3.797 06	4.115 65	4.502 83	4.883 42
8×8	1.176 82	2.614 26	2.879 04	**3.797 03**	**4.115 64**	**4.502 82**	4.883 18
9×9	1.176 82	2.614 26	2.879 04	3.797 03	4.115 64	4.502 82	**4.883 15**
10×10	1.176 82	2.614 26	2.879 04	3.797 03	4.115 64	4.502 82	4.883 15
			Antisymmetric modes about the centroidal-axis plane				
5×5	0.802 725	2.520 71	2.988 77	3.807 28	4.477 76	4.906 16	5.181 13
6×6	0.802 670	2.520 58	2.988 49	3.803 39	4.475 62	4.883 92	5.171 83
7×7	0.802 665	**2.520 56**	**2.988 47**	3.803 07	4.475 45	4.881 04	5.171 53
8×8	**0.802 664**	2.520 56	2.988 47	**3.803 03**	**4.475 44**	4.880 65	**5.171 51**
9×9	0.802 664	2.520 56	2.988 47	3.803 03	4.475 44	**4.880 60**	5.171 51
10×10	0.802 664	2.520 56	2.988 47	3.803 03	4.475 44	4.880 60	5.171 51

classified into two distinct categories: symmetric modes and antisymmetric modes about the centroidal-axis plane. If the angle θ is measured with respect to an axis within the centroidal-axis plane, then for the symmetric modes one has

$$F_s(\bar{r})=\cos[(s-1)\arccos(2\bar{r}-1)];$$
$$G_s(\theta)=\cos[(s-1)\theta]; \tag{16}$$
$$\bar{G}_s(\theta)=\sin(s\theta), \quad s=1,2,3,...,$$

and for the antisymmetric modes, one has

$$F_s(\bar{r})=\cos[(s-1)\arccos(2\bar{r}-1)]; \quad G_s(\theta)=\sin(s\theta);$$
$$\bar{G}_s(\theta)=\cos[(s-1)\theta], \quad s=1,2,3,.... \tag{17}$$

It can be seen that $F_s(\bar{r})$, $G_s(\theta)$, and $\bar{G}_s(\theta)$ in both Eqs. (16) and (17) are all orthogonal and complete series in the defined intervals.

Each of these two categories can be separately determined and thus it results in a smaller set of eigenvalue equations while maintaining the same level of accuracy.

III. CONVERGENCE STUDY

It is well known that eigenvalues provided by the Ritz method converge as upper bounds to the exact values. The solution of any accuracy can be obtained theoretically by using sufficient terms of admissible functions. However, there is a limit to the number of terms actually used in computation. Therefore, it is important to understand the convergence rate and the accuracy of the method. In the following convergence study, a thick torus with radius ratio $\bar{R}=R/a=1.5$ was used and in all the calculations, the Poisson's ratio $\nu=0.3$ was fixed. In most cases, optimal convergence could be obtained by using different number of terms in the component series of displacement functions. However, for simplicity, an equal number of terms in the Chebyshev polynomial series and the trigonometric series were used for every displacement function, i.e., $I=J=L=M=P=Q$, in the present analysis. Tables I and II show the convergence of the first seven eigenfrequency parameters $\Omega=\omega a\sqrt{\rho/G}$ for the circumferential wave number $n=1$ and $n=5$, respectively. Both the symmetric and antisymmetric modes were studied. Extensive convergence studies were also carried out for the axisymmetric vibration and the torsional vibration of the ring with the results shown in Table III and Table IV, respectively.

All the above computations were performed in double precision (16 significant figures) and piecewise Gaussian quadrature was used numerically to obtain the matrices in

TABLE IV. The convergence of eigenfrequencies of torsional vibration for a torus with circular cross section when $\bar{R}=1.5$.

Terms	Ω_1	Ω_2	Ω_3	Ω_4	Ω_5	Ω_6	Ω_7
			Symmetric modes about the centroidal-axis plane				
5×5	**2.260 99**	3.292 90	4.014 80	4.423 15	5.498 76	5.586 19	6.833 90
6×6	2.260 99	**3.292 68**	4.013 94	4.421 59	5.481 19	5.564 43	6.614 10
7×7	2.260 99	3.292 68	**4.013 94**	4.421 50	5.480 36	5.563 71	6.596 69
8×8	2.260 99	3.292 68	4.013 93	**4.421 49**	**5.480 32**	5.563 66	6.595 97
9×9	2.260 99	3.292 68	4.013 93	4.421 49	5.480 32	**5.563 65**	**6.595 92**
10×10	2.260 99	3.292 68	4.013 93	4.421 49	5.480 32	5.563 65	6.595 92
			Antisymmetric modes about the centroidal-axis plane				
5×5	**1.913 73**	3.266 34	4.410 64	5.411 69	5.525 28	6.617 86	6.837 02
6×6	1.913 73	**3.266 16**	4.409 75	5.397 88	5.523 02	6.597 85	6.829 73
7×7	1.913 73	3.266 16	**4.409 69**	5.397 56	5.522 41	6.596 06	6.818 01
8×8	1.913 73	3.266 16	4.409 69	**5.397 52**	5.522 40	6.595 91	6.817 95
9×9	1.913 73	3.266 16	4.409 69	5.397 52	**5.522 39**	**6.595 90**	**6.817 89**
10×10	1.913 73	3.266 16	4.409 69	5.397 52	5.522 39	6.595 90	6.817 89

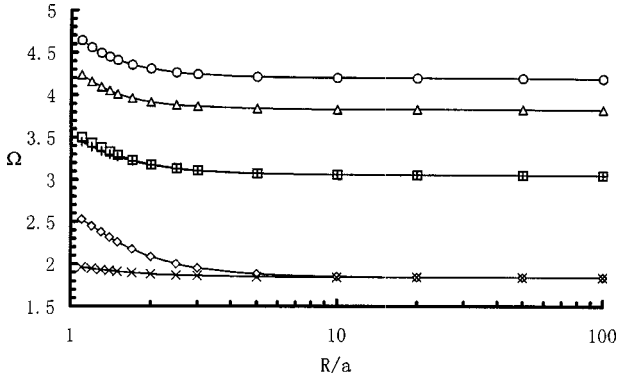

FIG. 2. The first six eigenfrequency parameters Ω of torsional vibration of a torus: $\diamond$, first symmetric mode; $\square$, second symmetric mode; $\triangle$, third symmetric mode; $\times$, first antisymmetric mode; $+$, second antisymmetric mode; $\bigcirc$, third antisymmetric mode.

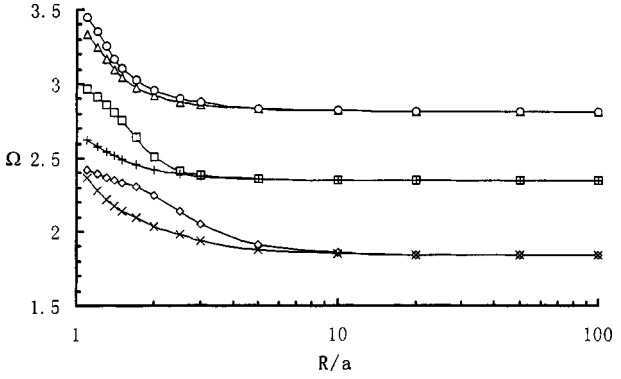

FIG. 4. The third to eighth eigenfrequency parameters Ω of a torus for circumferential wave number $n=1$: $\diamond$, second symmetric mode; $\square$, third symmetric mode; $\triangle$, fourth symmetric mode; $\times$, second antisymmetric mode; $+$, third antisymmetric mode; $\bigcirc$, fourth antisymmetric mode.

Eq. (15). It is seen that the first seven eigenfrequencies have converged monotonically to six significant figures by using only a few terms. As both the Chebyshev polynomial series and the trigonometric series are complete, one can conclude that these eigenfrequencies are ''exact values'' to six digits. Values given in boldface type and underlined are the converged values for the smallest number of terms used. Comparing Tables I and II, one can find that the convergence rate is almost the same for $n=1$ and $n=5$. The first seven eigenfrequencies accurate to six significant figures have been obtained by using only nine terms of the admissible functions in each coordinate.

IV. EIGENFREQUENCIES AND MODE SHAPES

The results for a torus with circular cross section are presented in Figs. 2–6, where the parameter R/a is plotted along a logarithmic axis. The ratio of the centroidal-axis radius to the cross-sectional radius varies from 1.1 to 100. Figure 2 shows the first six eigenfrequency parameters $\Omega = \omega a\sqrt{\rho/G}$ for torsional vibration, comprising three symmetric modes and three antisymmetric modes. The third to eighth eigenfrequency parameters Ω of axisymmetric vibration are given in Fig. 3, and they include the second to fourth symmetric modes and the second to fourth antisymmetric modes. Figure 4 gives the third to eighth eigenfrequency parameters Ω for the circumferential wave number $n=1$ that consist of the second to fourth symmetric modes and the second to fourth antisymmetric modes. From Figs. 2–4, it is seen that with the increase of the radius ratio R/a, the eigenfrequency parameters Ω of symmetric modes eventually coincide with those of antisymmetric modes. For a given cross-sectional radius a, the eigenfrequencies monotonically decrease with the increase of centroidal-axis radius R of the torus and approach certain constant values. In general, for $R/a>10$, we may consider the eigenfrequency parameters Ω to be constant.

The first and second eigenfrequencies of axisymmetric vibration, which correspond to the fundamental antisymmetric mode and symmetric mode, respectively, are described by a new eigenfrequency parameter $\Gamma=(R/a)\Omega=\omega R\sqrt{\rho/G}$. It is clear that both the torsional vibration and the axisymmetric vibration are independent of the coordinate θ. Torsional vibration is related to the coordinates φ and r while axisymmetric vibration is only related to the coordinate φ. In Fig. 5, six eigenfrequency parameters are shown for the fundamental symmetric and antisymmetric modes for circumferential wave number $n=1$, the second symmetric and antisymmetric modes for circumferential wave number $n=2$, as well as the fundamental symmetric and antisymmetric modes of axisym-

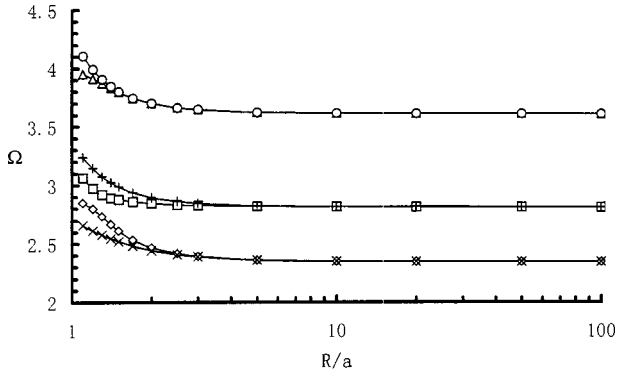

FIG. 3. The third to eighth eigenfrequency parameters Ω of axisymmetric vibration of a torus: $\diamond$, second symmetric mode; $\square$, third symmetric mode; $\triangle$, fourth symmetric mode; $\times$, second antisymmetric mode; $+$, third antisymmetric mode; $\bigcirc$, fourth antisymmetric mode.

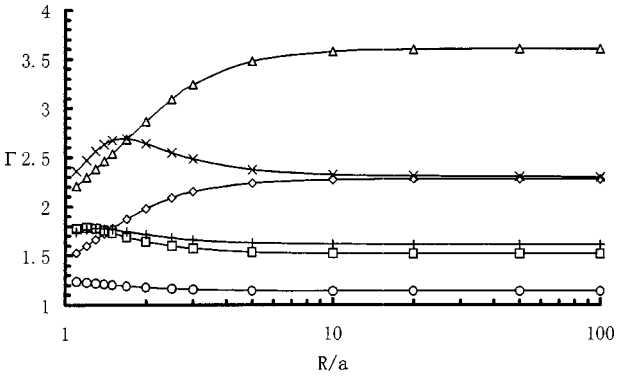

FIG. 5. Eigenfrequency parameters Γ of a torus for circumferential wave number $n\leqslant 2$ and for the axisymmetric vibration: $\diamond$, first symmetric mode for $n=1$; $\square$, first antisymmetric mode for $n=1$; $\triangle$, second symmetric mode for $n=2$; $\times$, second antisymmetric mode for $n=2$; $+$, first symmetric mode for axisymmetric vibration; $\bigcirc$, first antisymmetric mode for axisymmetric vibration.

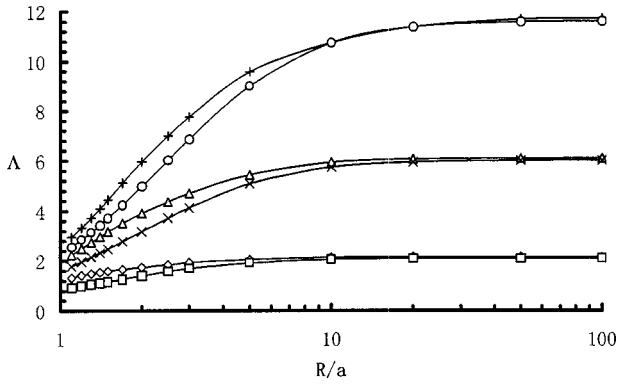

FIG. 6. The fundamental eigenfrequency parameters Λ of a torus for circumferential wave number $n \geqslant 2$: $\diamond$, first symmetric mode for $n=2$; $\square$, first antisymmetric mode for $n=2$; $\triangle$, first symmetric mode for $n=3$; $\times$, first antisymmetric mode for $n=3$; $+$, first symmetric mode for $n=4$; $\bigcirc$, first antisymmetric mode for $n=4$.

metric vibration. From the figure, one can find that the fundamental eigenfrequency parameter of symmetric modes for circumferential wave number $n=1$ and the second eigenfrequency parameter of symmetric modes for circumferential wave number $n=2$ monotonically increase with the increase of the radius ratio R/a. Among the rest, the eigenfrequency parameter of the first antisymmetric modes for axisymmetric vibration monotonically decreases with the increase of the radius ratio R/a. However, the others are not monotonic. In general, for $R/a>10$, we may also consider the eigenfrequency parameters Γ to be constant. In Fig. 6, the dimensionless parameter $\Lambda=(R/a)^2\Omega$ is used to describe the fundamental eigenfrequencies of a torus for circumferential wave number $n \geqslant 2$. In the figure, the fundamental eigenfrequency parameters of symmetric and antisymmetric modes for $n=2$, 3, 4 are plotted against the radius ratio R/a. It is seen that all the eigenfrequency parameters monotonically increase, and approach certain constant values with the increase of the radius ratio R/a. Moreover, with the increase of the radius ratio R/a, the eigenfrequencies of symmetric modes become close to those of antisymmetric modes.

In the above analysis, three different dimensionless eigenfrequency parameters Ω, Γ, and Λ are introduced, which facilitate not only the trends of the variation of eigenfrequencies but also a comparison with other solutions. In the approximate one-dimensional theory, the in-plane vibration and out-of-plane vibration of a ring are separately investigated. In Fig. 6, the symmetric modes correspond to the in-plane vibration solutions of the one-dimensional theory while the antisymmetric modes correspond to the out-of-plane vibration solutions. For example, according to the classical one-dimensional ring theory,[1,2] the eigenfrequencies for in-plane vibration of a circular ring are given by

$$\Lambda_{s-1}^2=0.65s^2(s^2-1)^2/(s^2+1), \quad s=2,3,4,\ldots, \tag{18}$$

and the eigenfrequencies for out-of-plane vibration are given by

$$\Lambda_{s-1}^2=0.65s^2(s^2-1)^2/(s^2+1+\nu), \quad s=2,3,4,\ldots. \tag{19}$$

A comparison of the present results with those obtained from the classical theory is given in Table V for a thin circular ring with the radius ratio $R/a=50$. It is shown that for thin circular rings, the classical theory can predict the lower-order eigenfrequencies with good accuracy. However, like all kinds of approximate theories, it cannot provide a full vibration spectrum of the circular ring and the error increases with the decrease of the radius ratio R/a. Moreover, the classical theory does not include shear deformation or rotary inertia effects. Taking a torus with the radius ratio $R/a=1.5$ as an example, the fundamental eigenfrequency parameter of in-plane vibration obtained by using the classical one-dimensional ring theory is $\Lambda_1=2.163\,33$. However, the corresponding eigenfrequency parameter obtained by using the present three-dimensional elasticity theory is $\Lambda_1=1.591\,17$. The error of the classical one-dimensional ring theory is up to about 36%! Considering the relations $\Lambda=(R/a)^2\Omega$ and $\Gamma=(R/a)\Omega$, and noting that $R/a>1$, one can find out from Figs. 2–6 by comparing Ω that for a torus, whether thin or thick, the lowest eigenfrequencies of both symmetric modes and antisymmetric modes are always those for $n=2$. Although the lower eigenfrequencies of a torus with large radius ratio R/a are confined to some particular modes, as seen from Fig. 6, for a torus with small radius ratio R/a, the lower eigenfrequencies for a larger variety of modes tend to cluster together, as is evident from Figs. 2–6.

Corresponding to each eigenfrequency, the three-dimensional deformed mode shapes of the torus can be easily obtained from Eqs. (13) and (15). As an example, the first three antisymmetric mode shapes and symmetric mode shapes of torsional vibration for a torus with radius ratio $R/a=1.5$ are given in Figs. 7 and 8 in contour form, respectively. It is known that for torsional vibration, the modes of the torus are the same at each cross section and only the deflection $W(r,\theta)$ in the circumferential direction φ exists. Therefore, only the mode shapes in a cross section need to be given.

TABLE V. A comparison of the eigenfrequency parameters Λ for a thin circular ring, $R/a=50$.

Methods	Λ_1	Λ_2	Λ_3	Λ_4	Λ_5	Λ_6
			In-plane vibration			
Present	2.162 23	6.110 11	11.7002	18.8898	27.6539	37.9700
Classical	2.163 33	6.118 82	11.7323	18.7938	27.8340	38.3099
			Out-of-plane vibration			
Present	2.099 17	6.016 84	11.5907	18.7688	27.5231	37.8296
Classical	2.101 21	6.029 06	11.6301	18.8651	27.7218	38.1955

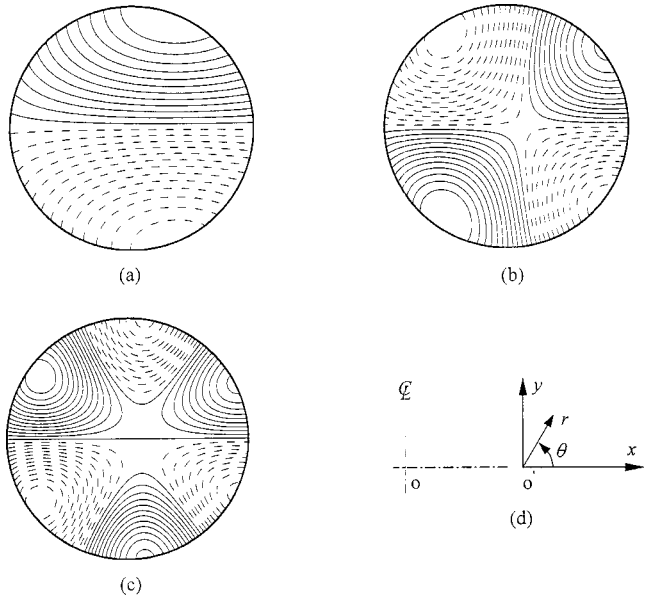

FIG. 7. The first three antisymmetric modes of torsional vibration when $R/a=1.5$: (a) the first mode; (b) the second mode; (c) the third mode; (d) coordinate system for the cross section.

V. CONCLUSIONS

This paper describes the detailed development of a three-dimensional analysis method for the free vibration of a torus with a circular cross section. The spatial integrals for strain and kinetic energy components have been formulated by developing a set of orthogonal coordinate systems. An energy functional has been defined and its extremum determined to arrive at the governing eigenfrequency equation. A combination of Chebyshev polynomials and trigonometric series are used as the admissible functions of the displacement components. The vibration of a torus is classified into three distinct categories, namely, axisymmetric vibration, torsional vibration, and vibration related to the circumferential wave number n. By using the symmetry of the structure, the vibration modes of every category are divided into symmetric and antisymmetric ones. This greatly reduces the computational cost while maintaining the same level of accuracy.

The convergence of eigenfrequencies has been examined. It is shown that the first seven eigenfrequencies accurate to at least six significant figures for each vibration type can be obtained by using only nine terms of the admissible functions. Through the parametric studies, the variation of eigenfrequencies versus the radius ratio of the torus is found. Important lower eigenfrequencies corresponding to general cross-sectional motions, which can only be determined by the three-dimensional elasticity theory, have been obtained. The present method is capable of determining eigenfrequencies and mode shapes very accurately. The results may serve as valuable benchmark solutions for validating the one-dimensional ring theories and new computational techniques for the problem.

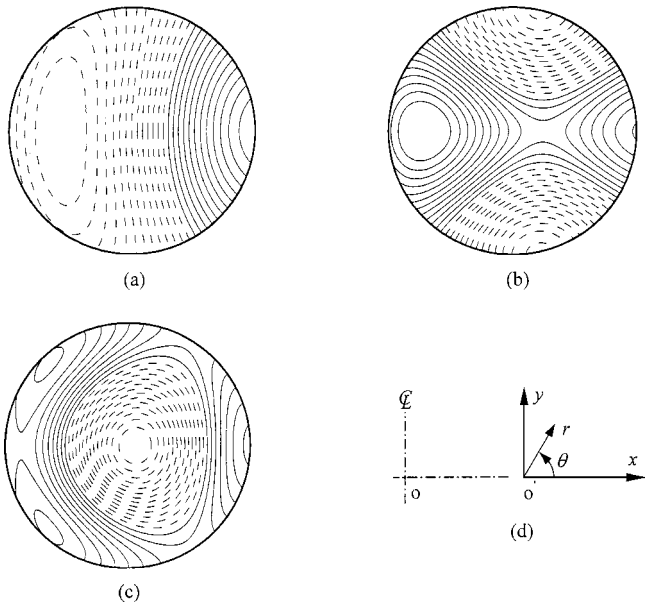

FIG. 8. The first three symmetric modes of torsional vibration when $R/a=1.5$: (a) the first mode; (b) the second mode; (c) the third mode; (d) coordinate system for the cross section.

ACKNOWLEDGMENTS

The work described in this paper was partially supported by a grant ''Analysis of building structures using hybrid stress hexahedral elements'' from the Research Grants Council of the Hong Kong Special Administrative Region, China (Project No. HKU7071/99E).

[1] A. E. H. Love, ''On the vibrations of an elastic circular ring (abstract),'' Proc. London Math. Soc. **24**, 118–120 (1892–1893).
[2] R. Hoppe, ''The bending vibration of a circular ring,'' Crelle J. Math. **73**, 158–168 (1871).
[3] S. S. Rao and V. Sundararajan, ''In-plane flexural vibrations of circular rings,'' J. Appl. Mech. **36**, 620–625 (1969).
[4] L. L. Philipson, ''On the role of extension in the flexural vibration of ring,'' J. Appl. Mech. **23**, 364–366 (1956).
[5] J. Kirkhope, ''Simple frequency expression of in-plane vibration of thick circular rings,'' J. Acoust. Soc. Am. **59**, 86–89 (1976).
[6] J. Kirkhope, ''Out-plane vibration of thick circular ring,'' J. Eng. Mech. **102**, 239–247 (1976).
[7] J. S. Bakshi and W. R. Callahan, ''Flexural vibrations of a circular ring when transverse shear and rotary inertia are considered,'' J. Acoust. Soc. Am. **40**, 372–375 (1966).
[8] C. S. Tang and C. W. Bert, ''Out-of-plane vibrations of thick rings,'' Int. J. Solids Struct. **23**, 175–185 (1987).
[9] O. Taniguchi and M. Endo, ''An approximate formula for the flexural vibration of a ring of rectangular cross section,'' Bull. JSME **14**, 348–354 (1971).
[10] A. W. Leissa, ''Vibration of shells,'' NASA SP-288, U.S. Govt. Printing Office, Washington, DC, 1973.
[11] P. Chidamparam and A. W. Leissa, ''Vibrations of planar curved beams, rings, and arches,'' Appl. Mech. Rev. **46**, 467–483 (1993).
[12] H. J. Ding and R. Q. Xu, ''Free axisymmetric vibration of laminated transversely isotropic annular plates,'' J. Sound Vib. **230**, 1031–1044 (2000).
[13] S. Srinivas, C. V. Rao, and A. K. Rao, ''An exact analysis for vibration of simply supported homogeneous and laminated thick rectangular plates,'' J. Sound Vib. **12**, 187–199 (1970).
[14] J. R. Hutchinson, ''Axisymmetric vibrations of a free finite-length rod,'' J. Acoust. Soc. Am. **51**, 233–240 (1972).
[15] J. R. Hutchinson, ''Vibration of solid cylinders,'' J. Appl. Mech. **47**, 901–907 (1980).
[16] J. R. Hutchinson, ''Transverse vibration of beams, exact versus approximate solutions,'' J. Appl. Mech. **48**, 923–928 (1981).

[17] J. R. Hutchinson, ''Vibrations of free hollow circular-cylinders,'' J. Appl. Mech. **53**, 641–646 (1986).
[18] J. R. Hutchinson, ''Vibrations of thick free circular plates, exact versus approximate solutions,'' J. Appl. Mech. **51**, 581–585 (1984).
[19] A. W. Leissa and J. So, ''Comparisons of vibration frequencies for rods and beams from one-dimensional and three-dimensional analysis,'' J. Acoust. Soc. Am. **98**, 2122–2135 (1995).
[20] J. So and A. W. Leissa, ''Three-dimensional vibrations of thick circular and annular plates,'' J. Sound Vib. **209**, 15–41 (1998).
[21] J. H. Kang and A. W. Leissa, ''Three-dimensional vibrations of thick, linearly tapered, annular plates,'' J. Sound Vib. **217**, 927–944 (1998).
[22] A. W. Leissa and J. H. Kang, ''Three-dimensional vibration analysis of thick shells of revolution,'' J. Eng. Mech. **125**, 1365–1371 (1999).
[23] J. H. Kang and A. W. Leissa, ''Three-dimensional vibrations of hollow cones and cylinders with linear thickness variations,'' J. Acoust. Soc. Am. **106**, 748–755 (1999).
[24] K. M. Liew, K. C. Hung, and M. K. Lim, ''A continuum three-dimensional vibration analysis of thick rectangular plates,'' Int. J. Solids Struct. **30**, 3357–3379 (1993).
[25] K. M. Liew, K. C. Hung, and M. K. Lim, ''Three-dimensional elasticity solutions to vibration of cantilevered skewed trapezoids,'' AIAA J. **32**, 2080–2089 (1994).
[26] K. M. Liew, K. C. Hung, and M. K. Lim, ''Vibration of thick prismatic structures with three-dimensional flexibilities,'' J. Appl. Mech. **65**, 619–625 (1998).
[27] C. W. Lim, K. M. Liew, and S. Kitipornchai, ''Vibration of open cylindrical shells: A three-dimensional elasticity approach,'' J. Acoust. Soc. Am. **104**, 1436–1443 (1998).
[28] K. M. Liew and Z. C. Feng, ''Vibration characteristics of conical shell panels with three-dimensional flexibility,'' J. Appl. Mech. **67**, 314–320 (2000).
[29] O. G. McGee and G. T. Giaimo, ''Three-dimensional vibrations of cantilevered right triangular plates,'' J. Sound Vib. **159**, 279–293 (1992).
[30] Y. K. Cheung and D. Zhou, ''Three-dimensional vibration analysis of cantilevered and completely free isosceles triangular plates,'' Int. J. Solids Struct. **39**, 673–687 (2002).
[31] J. H. Kang and A. W. Leissa, ''Three-dimensional vibrations of thick, circular rings with isosceles trapezoidal and triangular cross-section,'' J. Vibr. Acoust. **122**, 132–139 (2000).